Journal of Biomedical Optics

SPIEDigitalLibrary.org/jbo

Kinetics of red blood cell rouleaux formation studied by light scattering

Alicja Szołna-Chodór
Maciej Bosek
Bronisław Grzegorzewski

SPIE

Kinetics of red blood cell rouleaux formation studied by light scattering

Alicja Szołna-Chodór, Maciej Bosek, and Bronisław Grzegorzewski*
Nicolaus Copernicus University, Biophysics Department, Collegium Medicum in Bydgoszcz, ul. Jagiellońska 15, Bydgoszcz 85-067, Poland

Abstract. Red blood cell (RBC) rouleaux formation was experimentally studied using a light scattering technique. The suspensions of RBCs were obtained from the blood of healthy donors. Hematocrit of the samples was adjusted ranging from 1% to 4%. Measurements of the intensity of the coherent component of light scattered by the suspensions were performed and the scattering coefficient of the suspensions was determined. The number of RBCs per rouleaux was obtained using anomalous diffraction theory. The technique was used to show the effect of time, hematocrit, and sample thickness on the process. The number of cells per rouleaux first increases linearly, reaches a critical value at ~3 cells per rouleaux, and then a further increase in the rouleaux size is observed. The kinetic constant of the rouleaux growth in the linear region is found to be independent of hematocrit. The aggregation rate increases as the sample thickness increases. The time at which the critical region appears strongly decreases as the hematocrit of the suspension increases. [DOI: 10.1117/1.JBO.20.2.025001]

Keywords: red blood cells; rouleaux formation; coherent transmittance; anomalous diffraction theory.

Paper 140598RR received Sep. 18, 2014; accepted for publication Jan. 9, 2015; published online Feb. 3, 2015.

1 Introduction

Aggregation of red blood cells (RBCs) results in the formation of linear or branched structures called rouleaux. RBC aggregation is dependent both on plasma and cellular factors. The most important physiological consequence of the RBC aggregation is that the adhering of the cells significantly affects the rheological properties of blood.[1,2] Increased RBC aggregation has been observed in the pathophysiology of numerous diseases with circulatory disorders, such as cardiovascular diseases, inflammation, diabetes, hyperlipidemia, sickle cell disease, thalassemia, and trauma.[3] Because of this, many techniques were utilized to fully elucidate the specific mechanisms involved in RBC aggregation. Analysis of the light scattering by RBC aggregates is one of the most popular.

Various theoretical approaches have been applied to describe light scattering by RBC aggregates.[4–7] The optical properties of individual RBCs that have been well recognized[8–15] are usually a starting point in the study. Tsinopoulos et al.[4] calculated light scattering by rouleaux (up to 8 RBCs per rouleaux) giving the differential scattering cross section of the units. Shvartsman and Fine[5] described an effect of RBC aggregation on the transparency of blood using anomalous diffraction theory, which was previously utilized by Twersky[9] in the study of scattering by biological suspensions. He et al,[7] using finite-difference time-domain method, calculated scattering probability for multiple RBCs that may be a model of rouleaux. Additionally, the data obtained in the study of the optical properties of blood[11] allowed interpretation of optical coherence tomography signals from sedimenting RBCs.[16] Pop and Neamtu[6] studied the diffuse component of light scattered in suspension of aggregating RBCs. Using Mie theory, they determined the number of RBCs per aggregate as functions of time and hematocrit.

RBC aggregation causes an increase in transmitted light intensity, whereas the intensity of the reflected light decreases in the course of aggregation.[17] The extensive study in the area has been performed and on this basis, study instruments for the measurement of RBC aggregation have been developed e.g., Myrenne RBC aggregometer,[18] laser-assisted optical rotational cell analyzer,[19] RheoScan-A,[20] and Sefam erythroaggregometer.[21–23] The parameters obtained from the instruments reflect the kinetics of the RBC aggregation. However, those instruments do not allow estimation of the number of RBCs per aggregate.[24]

To explain the RBC aggregation, two opposite models have been developed. Within the bridging model, bridging forces due to plasma proteins adsorbed on the RBC membrane cause the adhering of the cells. In contrast, according to the depletion model, depletion forces due to decreasing of the protein concentration in the vicinity of the cell membrane contribute to the aggregation. Recently, both the theoretical study[25] as well as the experimental investigations[26] seem to confirm the depletion model of the aggregation. The nature and magnitude of the interactive forces between the RBCs manifests in the kinetics of the RBC aggregation. Many techniques for the assessment of the kinetics of RBC aggregation have been developed. The quantitative methods of description of these kinetics are particularly needed in clinical diagnostics.

The kinetics of rouleaux formation has been studied both theoretically and experimentally. One of the first approaches to the study of RBC aggregation was done by Ponder.[27] Using a microscopic technique, he determined the number of cells in rouleaux that appear at a given time in a dilute

*Address all correspondence to: Bronisław Grzegorzewski, E-mail: grzego@cm.umk.pl

0091-3286/2015/$25.00 © 2015 SPIE

suspension of the cells at various temperatures. Ponder has shown that the Smoluchowski theory of colloid aggregation describes the size distribution of the rouleaux very well. Furthermore, Ponder argued that for small aggregates, the mean rouleaux size increases linearly with time. The investigations developed by Kernick et al.[28] for various temperatures and hematocrits have shown that after a linear increase in the rouleaux length a nonlinear increase appears. They have confirmed Ponder's finding that Smoluchowski theory is adequate for small rouleaux. Samsel and Perelson[29] formulated a theory of the kinetics of rouleaux formation taking into account both irreversible as well as reversible reactions. Making a comparison between the theory and results obtained by Kernick et al.[28] Samsel and Perelson[29] argued that the kinetics of rouleaux formation is a result of reversible reactions. A new insight in the problem was done by Barshtein et al.[30] Using microscopic techniques, they investigated the rouleaux formation in a narrow gap flow chamber at small hematocrits. Especially, they have shown detailed results related to the kinetics of spontaneous rouleaux formation. They confirmed that in the initial stage of the process, the average aggregate growth is a linear function of time. However, after the initial stage, a critical region of slow growth was observed and the aggregate size strongly increased with time. Barshtein et al.[30] have shown that in the initial stage, the irreversible reactions of polymerization and condensation take place. The study of the kinetics performed by Shiga et al.[31] using a rheoscope and image analyzer has shown that at the shear rate 7.5 s^{-1}, the rate of rouleaux formation is proportional to hematocrit within the range from 0.1% to 0.6%. Moreover, they have shown an increase in the rate of rouleaux formation with the depth of the sample.

In this paper, the kinetics of the rouleaux formation was investigated by light scattering. Diluted suspensions of RBCs in autologous plasma were obtained from the blood of healthy donors. The intensity of the coherent component of light was measured at various hematocrits as a function of time and sample thickness. From the experimental data, the scattering coefficient of RBC suspensions was determined. The anomalous diffraction theory was used to calculate the scattering cross section of the rouleaux and the average number of erythrocytes per rouleaux. Finally, the kinetics of the rouleaux formation is described.

2 Materials and Methods

2.1 *Sample Preparation*

Venues blood was drawn from adult healthy donors from a local blood center into K_3EDTA anticoagulant and stored at 4°C. The whole blood was centrifuged at 3000 rpm for 5 min at 4°C, then the plasma was separated and the buffy coat was discarded. To remove any remains, RBCs were washed three times in 0.9% saline at previous settings of the centrifuge. To eliminate the remains of RBCs and WBCs, the plasma was centrifuged at 15,000 rpm for 15 min at 11°C. Next the plasma was combined with autologous RBCs with hematocrits 1% to 4%. Samples were gently shaken for 60 s to obtain the individual RBCs. Suspensions were injected into the wedge-shaped container. Experiments were made at room temperature (21°C). In our investigations, 70 samples were tested, 10 for each hematocrits. The experiment was carried out according to the ethical guidelines laid down by the local bioethical commission.

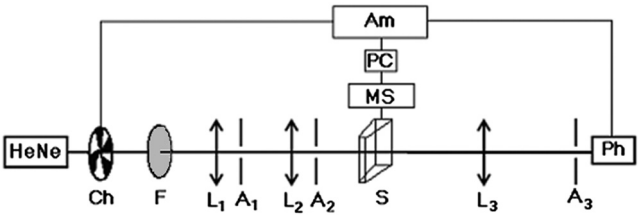

Fig. 1 Scheme of the experimental setup: HeNe—laser, Ch—chopper, F—filter, L_1-L_3—lenses, A_1-A_3—apertures, S—sample, Ph—photomultiplier, Am—amplifier, PC—computer, MS—motorized stage.

2.2 *Coherent Component of Light Measurements*

The experimental setup for this study is schematically shown in Fig. 1. The He–Ne laser at a wavelength of 632.8 nm is used as a light source. The laser light is collimated by the lenses L_1 and L_2, and selected by the pinhole P_1, which plays the part of a spatial filter. The beam of light is passing through the aperture A_1. Next, the light is scattered in the sample S in the wedge-shaped container, which is moved on its horizontal axis by motorized stage MS. The coherent component of light is selected using lens L_3 and aperture A_2. The photomultiplier Ph is used as detector of intensity of the coherent component of light, and the signal is amplified and stored in a computer. To reduce the noise, the chopper Ch is used in conjunction with the amplifier (Am). During each scanning cycle, the data are collected for sample thicknesses from 0.2 to 0.4 mm.

2.3 *Theoretical Background of Light Scattering by Red Blood Cell Suspension*

In the suspension of RBCs illuminated by He–Ne laser light at the wavelength of 632.8 nm, the scattering is dominant over absorption.[8] According to the theory of absorption and scattering given by Twersky, the total transmittance is a sum of the coherent component and incoherent component.[9] The coherent part of the transmittance C, called the collimated transmittance, has the form

$$C(t) = \exp[-\mu_s(t)d], \tag{1}$$

where $\mu_s(t)$ is the macroscopic scattering coefficient of the suspension and d is the thickness of the sample. Due to the aggregation process, the scattering coefficient $\mu_s(t)$ is a function of time. This macroscopic coefficient is related with the cross section of the rouleaux $\sigma_s(t)$ by the expression

$$\mu_s(t) = \frac{\sigma_s(t)H(1-H)}{V_u(t)}, \tag{2}$$

where $V_u(t)$ is the volume of the rouleaux and H is the hematocrit.

The relative index of refraction (refractive index of RBC per refractive index of the plasma) at the wavelength of the incident radiation 632.8 nm is about 1.04. We assume that RBCs as well as rouleaux can be modeled as spherical particles. Furthermore, we assume that rouleaux have the same relative index of refraction as the index for RBC. Indeed, we assume that the rouleaux consist of tightly packed cells. Under these assumptions, the anomalous diffraction theory can be used to estimate the scattering cross section $\sigma_s(t)$ of the units. The scattering cross section $\sigma_s(t)$ of the units is equal to[32]

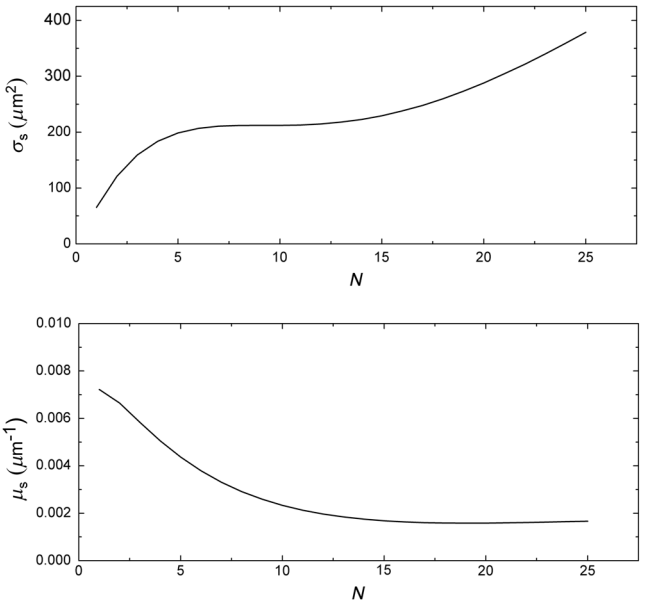

Fig. 2 The scattering cross section σ_s (a) and scattering coefficient μ_s (b) as a function of the number of cells per rouleaux.

$$\sigma_s(t) = \pi r_u^2(t)\left\{2 - \frac{4}{\rho(t)}\sin\rho(t) + \frac{4}{\rho^2(t)}[1-\cos\rho(t)]\right\}, \tag{3}$$

where

$$\rho(t) = \frac{4\pi r_u(t)}{\lambda}(n-1). \tag{4}$$

In the above equation, $r_u(t)$ is the radius of the unit at the time t, n is the relative index of refraction and λ is the wavelength of the radiation in the medium. Figure 2(a) shows the scattering cross section as a function of the number of the cells per rouleau. The parameters shown in Fig. 2 were calculated at the wavelength $\lambda = 632.8$ nm, relative index of refraction $n = 1.04$, and the volume of single cell $V = 90\ \mu m^3$ which corresponds to the radius of the sphere $r = 2.78\ \mu$m. The scattering coefficient was calculated at the hematocrit of the suspension $H = 0.01$. The functions were calculated in the interval $1 \le N \le 25$. The anomalous diffraction theory gives the scattering cross section of the single cell $\sigma_s = 65.58\ \mu m^2$, which corresponds to that obtained by Steinke and Shepherd from Mie theory $\sigma_s = 66.62\ \mu m^2$.[8] The cross section nonlinearly increases as the number of the cells per rouleaux increases. The scattering coefficient first decreases as the number of the cells per rouleaux increases and at $15 > N$ takes almost constant values. This

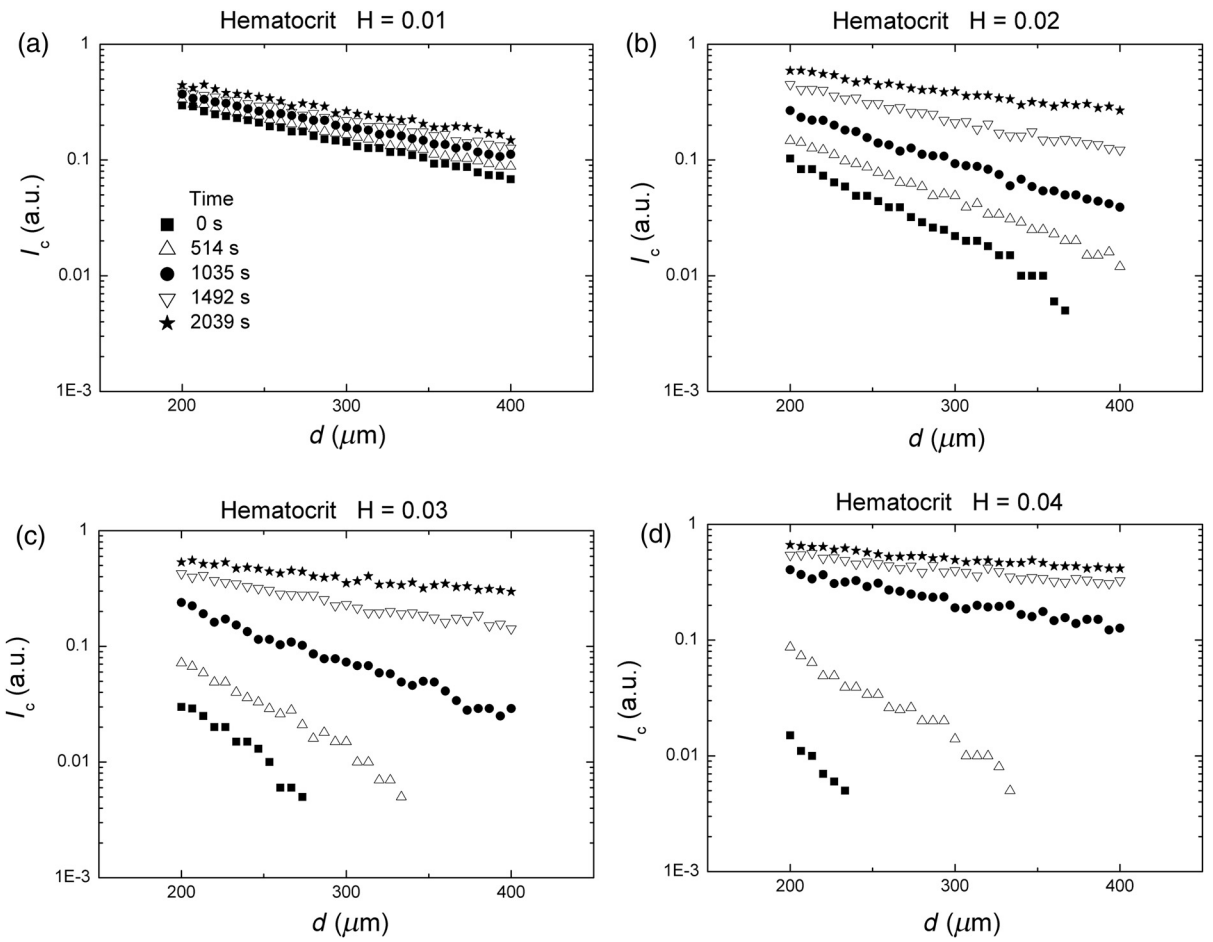

Fig. 3 The dependence of the intensity of the coherent component I_c on the thickness d of the sample and time t, for hematocrit (a) 0.01, (b) 0.02, (c) 0.03 and (d) 0.04. Each scanning cycle is displayed with the time that the cycle began.

means that in this case the inverse scattering problem can be resolved at $N < 15$. Another restriction for the inverse scattering problem is the combination of the number of the cells per rouleaux, hematocrit of the suspension, and the thickness of the sample. Especially at large values of $\mu_s d$, the diffuse component of light increases and it may be difficult to separate the coherent component from the diffuse component.

3 Results

The effect of rouleaux formation on the intensity of the coherent component for four hematocrits is depicted in Fig. 3. At every hematocrit, the data for five scanning cycles are presented, and the time for the beginning of each cycle is denoted. The intensity during each scanning cycle is a function of the thickness of the sample and the time. The increase of the intensity in time is a result of the aggregation process. The slope of the intensity in the logarithmic scale systematically decreases with time. The results show that the changes of the intensity depend on the hematocrit of the samples. At the hematocrit 0.01, the temporal increase of the intensity is relatively small as compared to the increase at hematocrit 0.04. Furthermore, at higher hematocrits after a fast increase of the intensity at the early stages of the aggregation, much slower increase of the intensity can be observed.

The slope of the intensity versus sample thickness is used to determine the scattering coefficient of the suspensions. To find the effect of the sample thickness on the aggregation process, the slope is analyzed in two regions of the sample thickness: 200 μm < d < 300 μm and 300 μm < d < 400 μm. The intensity at various sample thicknesses at given scanning cycles was measured in different times. We have assumed that within the time necessary to performance one scanning cycle the state of the aggregation of the cells does not substantially change.

Figure 4 shows the effect of hematocrit and sample thickness on the macroscopic scattering coefficient $\mu_s(t)$ of the RBC suspension. The decrease of the scattering coefficient with time manifests the aggregation of the cells. Figure 4 shows a little difference in the temporal behavior of the scattering coefficient at the two intervals of sample thickness. For the higher hematocrit, the scattering coefficient was not determined for initial times at the sample thickness 300 μm < d < 400 μm, because at this thickness, the intensity of the coherent component takes very small values.

The number of cells per aggregate at a given instant of time was numerically determined from the experimental data of the scattering coefficient using Eqs. (2) and (3). The number of cells per aggregate is shown in Fig. 5. For every hematocrit, 10 samples were taken from different donors. Thus, the error bars showing standard deviations reflect the subject to subject variability in the number of cells per aggregate. The time course of the aggregate formation has a common feature independent on the hematocrit of the samples. In the first stage of the process, the linear increase in the number of cells per aggregate takes place. Next, a critical region appears when aggregates take a constant size of about three erythrocytes. Finally, a further increase in the number of the cells can be observed. Critical

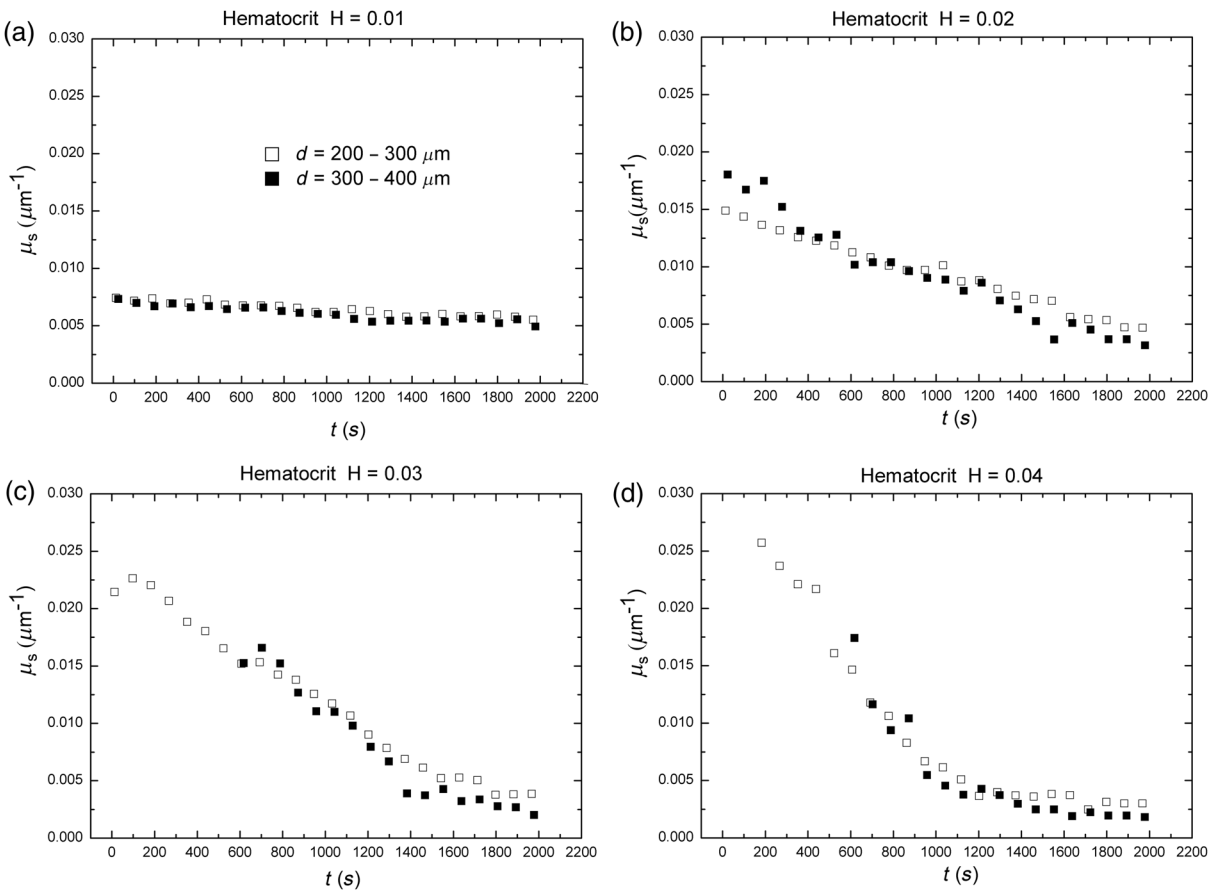

Fig. 4 The dependence of the scattering coefficient μ_s on time at the thickness interval 200 μm < d < 300 μm (empty squares) and 300 μm < d < 400 μm (filled squares) for hematocrit (a) 0.01, (b) 0.02, (c) 0.03 and (d) 0.04.

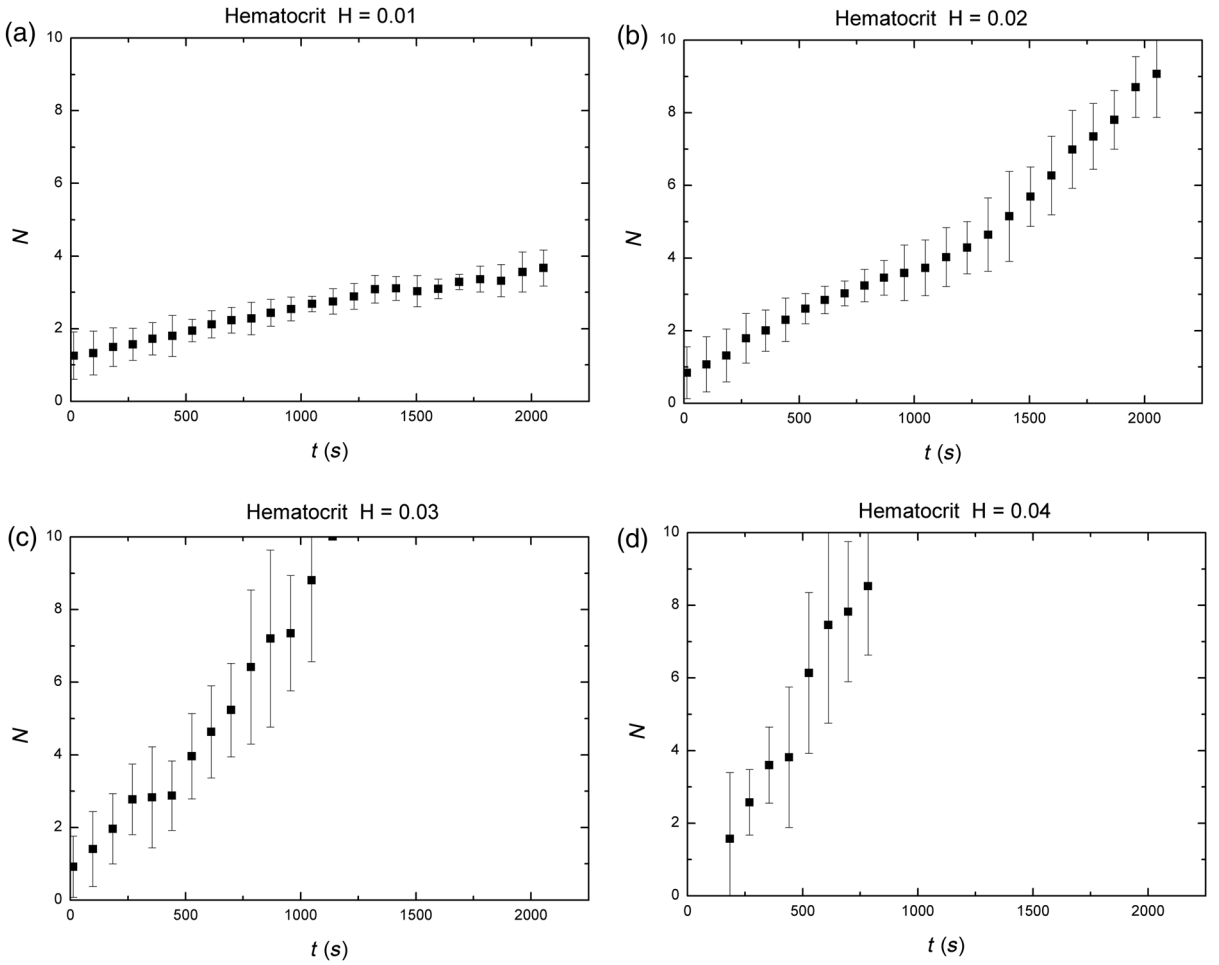

Fig. 5 The number of red blood cells (RBCs) per aggregate N as a function of time at hematocrit (a) 0.01, (b) 0.02, (c) 0.03, and (d) 0.04 obtained at the sample thickness 200 μm < d < 300 μm.

size is found as a median between the last point of initial linear increase and the first point of further growth.

Figure 6 shows the aggregate size in the critical region separating two regions of aggregate growth for the investigated hematocrit. It is seen that, independent of the hematocrit, the above defined critical size is equal to 3 ± 0.5 erythrocytes.

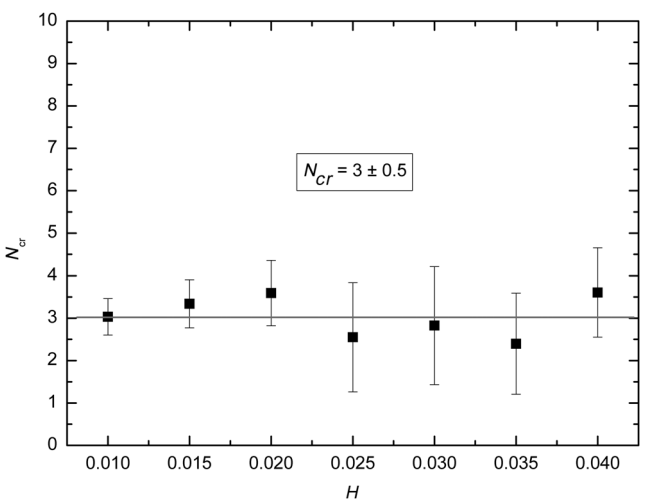

Fig. 6 The critical size N_{cr} as a function of hematocrit obtained at the sample thickness 200 μm < d < 300 μm.

Figure 7 shows an effect of the sample thickness on the aggregation process. In this figure, the means of the number of cells per aggregate are shown and the standard deviation is omitted for clarity. The results show that the aggregation rate is a little higher at the sample thickness 300 μm < d < 400 μm as compared to the rate at the thickness 200 μm < d < 300 μm.

To show the effect of hematocrit on the kinetics of the rouleaux formation, the aggregation rate was calculated for the first stage of the process. The aggregation rate is defined as $\Delta N/\Delta t$, where N is the number of RBCs per rouleaux and t denotes the time. Figure 8 shows the aggregation rate in the first stage of the process as a function of hematocrit of the samples at the two sample thickness intervals.

The results obtained in this paper can be compared with the results obtained with the use of the microscopic technique by Kernick et al.[28] In the comparison shown in Fig. 9, we have taken into account the number of RBCs per rouleaux that appears at 600 s at various hematocrits of the samples. A comparison of the results shows that the numbers of cells per rouleaux obtained from the scattering technique are in quite good agreement with ones obtained from the microscopic technique. Especially, it can be seen that the number of cells per rouleaux first increases with the increase of the hematocrit, then for a short hematocrit range takes a constant critical size and finally increases more.

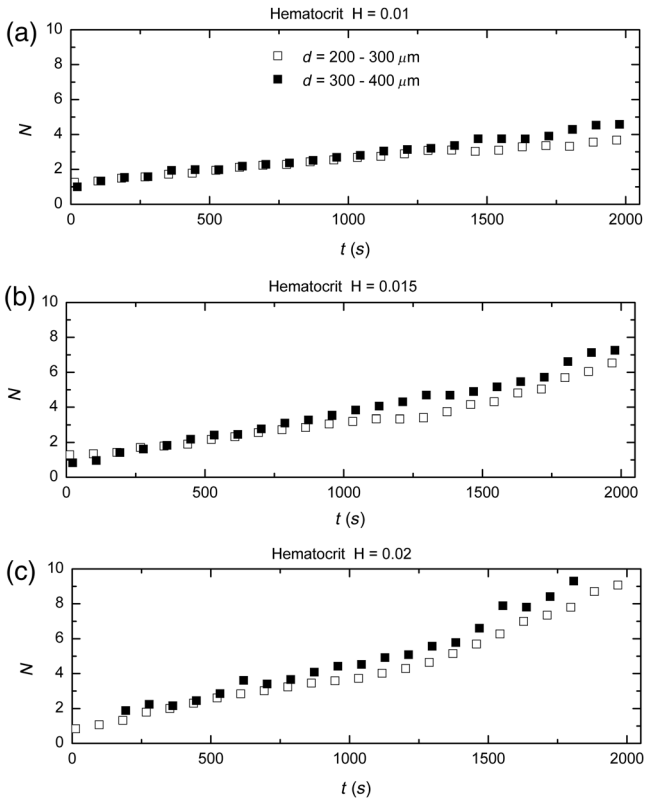

Fig. 7 An effect of sample thickness on the kinetics of the rouleaux formation. The number of RBCs per aggregate N as a function of time at hematocrit (a) 0.01, (b) 0.015, (c) 0.02 obtained at the sample thickness 200 μm < d < 300 μm (empty squares) and 300 μm < d < 400 μm (filled squares).

Figure 10 schematically shows isolines of equal numbers of RBCs per rouleaux that appear at a given time at various hematocrits. This figure is, indeed, a phase diagram of the RBC suspension. The lines were found as an estimation of the experimental data. The low coherent part of the transmittance at the beginning of the process for hematocrit above 0.03 does not allow a good description of these lines in the right bottom corner of this figure. The line which represents the dependence of the critical size ($N = 3$) on hematocrit divides the

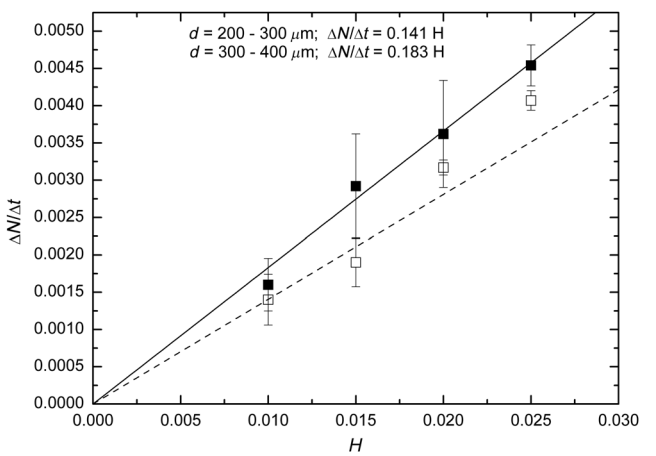

Fig. 8 The dependency of the rate of aggregation $\Delta N/\Delta t$ on hematocrit in intervals 200 μm < d < 300 μm (empty squares) and 300 μm < d < 400 μm (filled squares).

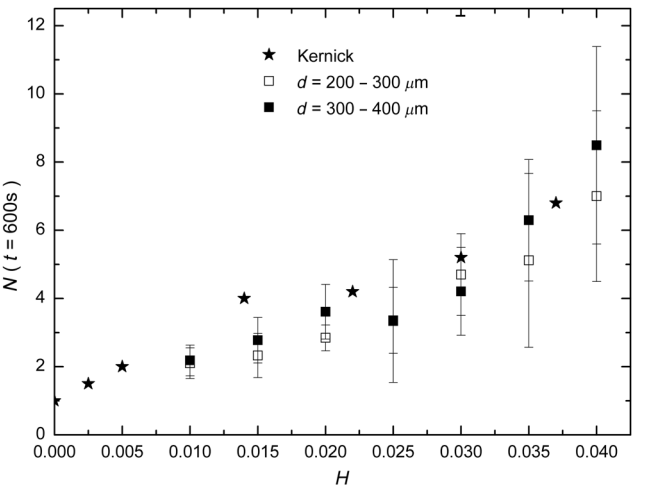

Fig. 9 Dependence of the number of the cells per rouleaux N at t = 600 s on hematocrit. Empty squares represent results from depth interval 200 μm < d < 300 μm, filled squares represent results from interval 300 μm < d < 400 μm and stars represent the result obtained by Kernick et al.[28]

diagram into two parts. Above the critical line, the density of isolines is much larger than below. This shows that up to three RBC per rouleaux growth of rouleaux are slower than they are later. Below the critical line, linear growth of the rouleaux takes place. A critical region divides the plot into regions of slower and faster aggregate growth. Thus, any vertical line in this diagram represents the growth of the aggregates with time at a given hematocrit, allowing the observation of the kinetics of their formation. On the other hand, any horizontal line in the diagram represents observation of the RBC suspensions in a fixed time at various hematocrits. In this way, the results shown in Fig. 9 correspond to the line $t = 600$ s in Fig. 10. Both the results obtained from the scattering experiment as well as the ones obtained by Kernick et al. shown in Fig. 9 reflect the characteristic three regions of the phase diagram very well. In this case, the growth of aggregate size with

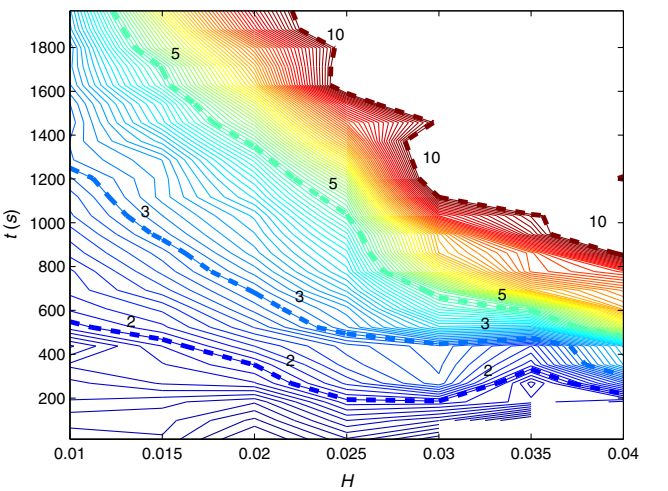

Fig. 10 Isolines of the number of RBCs per averaged rouleaux for the sample thickness 200 μm < d < 300 μm. The solid lines are incremented by 0.1 RBC. Four dashed lines represent the isolines for 2, 3, 5, and 10 erythrocytes.

increasing hematocrit for given time as well as with increasing time for given hematocrit is intermediated by critical region.

4 Discussion

Although the study of the kinetics of RBC aggregate formation has a long history, there is no commonly accepted theory that describes the process. The results shown in this paper, together with others, support the thesis that in the early stage of rouleaux formation, the number of RBCs per rouleaux grows linearly in time. Duration of the stage of linear growth can be observed up to the time when aggregates attain the critical region. The linear growth was first postulated by Ponder,[27] where he showed that Smoluchowski's theory of irreversible coagulation of colloids permits one to predict the distribution of the number of the cells per relatively short rouleaux. Kernick et al.[28] have found that the kinetics of the aggregation becomes nonlinear with time, but confirmed Ponder's conclusions about the size distribution for a small rouleaux length. The detailed experimental evidence of the linear growth was presented by Barshtein et al.[30] and they have shown that the polymer formation model developed by Samsel and Perelson[29] can be adopted to explain the early stage of the RBC aggregation. Furthermore, they have shown that the process is performed by polymerization and condensation at equal constants of the interactions. The results presented in this paper support the model of the early spontaneous aggregation of RBCs. Furthermore, our results confirm only the thesis that the early stage of linear growth involves aggregation of a few cells.

One of the most important features of the rouleaux formation kinetics is the presence of the critical region that appears when rouleaux attain a critical size of about three erythrocytes. The critical region is followed by the region of further growth in size. The phenomenon was observed for the first time by Barshtein et al.[30] and the dependence of the critical time on hematocrit was found. Thus, from one side, the results presented in this paper confirm the findings of Barshtein et al.[30] and, from the other side, explain data obtained by Kernick et al.[28] Among the studies of the kinetics performed by Samsel and Perelson, the critical region was not found but it was shown that reversible reactions may lead to a state of saturation. Taking into account the reversible reactions, Samsel and Perelson[29] argued that data obtained by Kernick et al.[28] can be explained within the theory. In opposition to the conclusions drawn from the reversible reaction theory, we have shown that after the critical region, further growth of the aggregate size appeared. Further growth of aggregates after deviation from linearity was also observed by Barshtein et al.[30] The conclusion of Samsel and Perelson[29] comes from the fact that due to the limited number of data points and the short times of observations (up to 1 h) performed by Kernick et al.,[28] the critical region was recognized as a steady state. An extrapolation of results from Fig. 10 shows that at the $H = 0.005$, the critical region is reached after about 50 min. A tentative explanation of the problem seems to be as follows: the initial linear growth of the rouleaux can be described by the polymer formation model. This model works up until the mean rouleaux length does not exceed the critical size. Formation of the small rouleaux undergo via face-to-face interactions because the reactive area of the wall of the existing rouleaux is much less than the area of their face. When the mean rouleaux length exceeds the critical size, the reactive area of the wall is comparable to or higher than the area of the face which results in enhanced aggregation. Thus, the results shown in this paper seem to support the thesis that after a linear growth of the rouleaux, the critical region followed by further growth of the aggregates appears.

As was mentioned above, we have found that the critical time is strongly dependent on hematocrit. There is a great difference in the critical time measured by Barshtein et al.[30] and the time when the critical regions begins in this study. The values of the time obtained in this study are about 10 times larger those that obtained by Barshtein et al.[30] Note that Barshtein et al.[30] measured the aggregation in a flow chamber having a 40-μm gap while our measurements were performed in a vertically oriented container having a thickness between 200 and 400 μm.

Finally, let us consider the comparison of the result obtained in this study with the results presented by Kernick et al.[28] It was shown for the first time, to our knowledge, that results obtained with the light scattering technique are in very good agreement with results obtained from the microscopic technique. Thus, this unexpected result of the study shows that the proposed light scattering technique may be promising in the study of RBC aggregation.

5 Conclusion

In this study, the light scattering technique was successfully used to investigate the RBC aggregate suspension, which was mainly studied using a microscopic technique up until now. It was shown that for these suspensions, the anomalous diffraction theory can be used. Using a theoretical expression for the scattering coefficient, the scattering cross section and the size of the aggregates was obtained. The evolution in time of this size was observed. Three phases of this evolution were found. Initially, the linear increase of their size can be observed. Next, when aggregates gain an average size of about three erythrocytes, the critical region appears. Finally, further growth of their size takes place. Furthermore, the investigations show the dependence of the observed phenomena on hematocrit and sample thickness. The phases of aggregate evolution were detailed and described with the use of a phase diagram. This new approach indicates the need for a more detailed model of RBC aggregation in the early stage.

References

1. J. J. Bishop et al., "Rheological effects of red blood cell aggregation in the venous network: a review of recent studies," *Biorheol.* **38**, 263–274 (2001).
2. A. S. Popel and P. C. Johnson, "Microcirculation and hemorheology," *Annu. Rev. Fluid Mech.* **37**, 43–69 (2005).
3. T. Shiga, N. Maeda, and K. Kon, "Erythrocyte rheology," *Crit. Rev. Oncol. Hematol.* **10**(1), 9–48 (1990).
4. S. V. Tsinopoulos, E. J. Sellountos, and D. Polyzos, "Light scattering by aggregated red blood cells," *Appl. Opt.* **41**(7), 1408–1417 (2002).
5. L. D. Shvartsman and I. Fine, "Optical transmission of blood: effect of erythrocyte aggregation," *IEEE Trans. Biomed. Eng.* **50**(8), 1026–1033 (2003).
6. C. V. L. Pop and S. Neamtu, "Aggregation of red blood cells in suspension: study by light-scattering technique at small angle," *J. Biomed. Opt.* **13**(4), 041308 (2008).
7. J. He and A. Karlsson, "Light scattering by multiple red blood cells," *J. Opt. Soc. Am. A* **21**(10), 1953–1961 (2004).
8. J. M. Steinke and A. P. Shepherd, "Comparison of Mie theory and the light scattering of red blood cells," *Appl. Opt.* **27**(19), 4027–4033 (1988).
9. V. Twersky, "Absorption and multiple scattering by biological suspensions," *J. Opt. Soc. Am.* **60**(8), 1084–1093 (1970).

10. M. Hammer et al., "Single scattering by red blood cells," *Appl. Opt.* **37**(31), 7410–7418 (1998).
11. A. Roggan et al., "Optical properties of circulating human blood in the wavelength range 400–2500 nm," *J. Biomed. Opt.* **4**(1), 36–46 (1999).
12. M. Friebel et al., "Determination of optical properties of human blood in the spectral range 250 to 1100 nm using Monte Carlo simulations with hematocrit-dependent effective scattering phase functions," *J. Biomed. Opt.* **11**(3), 034021 (2006).
13. M. Friebel et al., "Influence of shear rate on the optical properties of human blood in the spectral range 250 to 1100 nm," *J. Biomed. Opt.* **12**(5), 054005 (2007).
14. P. Mazeron et al., "A theoretical approach of the measurement of osmotic fragility of erythrocytes by optical transmission," *Photochem. Photobiol.* **72**(2), 172–178 (2000).
15. J. Didelon et al., "Osmotic fragility of the erythrocyte membrane: characterization by modeling of the transmittance curve as a function of the NaCl concentration," *Biorheol.* **37**(5–6), 409–416 (2000).
16. M. Y. Kirillin et al., "Effect of red blood cell aggregation and sedimentation on optical coherence tomography signals from blood samples," *J. Phys. D Appl. Phys.* **38**, 2582 (2005).
17. W. G. Zijlstra, "Syllectometry, a new method for studying rouleaux formation of red blood cells," *Acta. Physiol. Pharmacol. Neerl.* **7**, 153–154 (1958).
18. H. Schmid-Schönbein, "Apparatus for measuring the aggregation rate of particles," U.S. Patent No. 4135819 (1977).
19. M. R. Hardeman et al., "Laser-assisted optical rotational cell analyser (LORCA.); I. A new instrument for measurement of various structural hemorheological parameters," *Clin. Hemorheol. Microcirc.* **14**(4), 605–618 (1994).
20. S. Shin, Y. Yang, and J.-S. Suh, "Measurement of erythrocyte aggregation in a microchip stirring system by light transmission," *Clin. Hemorheol. Microcirc.* **41**(3), 197–207 (2009).
21. J. F. Stoltz, F. Paulus, and M. Donner, "Experimental approaches to erythrocyte aggregation," *Clin. Hemorheol.* **7**, 109–118 (1987).
22. A. V. Priezzhev et al., "Aggregation and disaggregation of erythrocytes in whole blood: study by backscattering technique," *J. Biomed. Opt.* **4**(1), 76–84 (1999).
23. M. J. Pearson and H. H. Lipowsky, "Effect of fibrinogen on leukocyte margination and adhesion in postcapillary venules," *Microcirculation* **11**(3), 295–306 (2004).
24. O. K. Baskurt et al., "Comparison of three instruments for measuring red blood cell aggregation," *Clin. Hemorheol. Microcirc.* **43**(4), 283–298 (2009).
25. B. Neu, S. O. Sowemimo-Coker, and H. J. Meiselman, "Cell-cell affinity of senescent human erythrocytes," *Biophys. J.* **85**(1), 75–84 (2003).
26. P. Steffen, C. Verdier, and C. Wagner, "Quantification of depletion-induced adhesion of red blood cells," *Phys. Rev. Lett.* **110**, 018102 (2013).
27. E. Ponder, "On sedimentation and rouleaux formation—II," *Exp. Physiol.* **16**, 173–194 (1926).
28. D. Kernick et al., "Experiments on rouleau formation," *Can. J. Physiol. Pharm.* **51**(9), 690–699 (1973).
29. R. W. Samsel and A. S. Perelson, "Kinetics of rouleau formation. II. Reversible reactions," *Biophys. J.* **45**(4), 805–824 (1984).
30. G. Barshtein, D. Wajnblum, and S. Yedgar, "Kinetics of linear rouleaux formation studied by visual monitoring of red cell dynamic organization," *Biophys. J.* **78**(5), 2470–2474 (2000).
31. T. Shiga et al., "Kinetics of rouleaux formation using TV image analyzer. I. Human erythrocytes," *Am. J. Physiol.* **245**(2), H252–H258 (1983).
32. H. C. Van de Hulst, *Light Scattering by Small Particles*, John Wiley & Sons, New York (1957).

Alicja Szołna-Chodór received her MS degree in physics from Nicolaus Copernicus University, Faculty of Physics, Astronomy and Informatics in 2006. Currently, she is a research scientist and university teacher at Ludwik Rydygier Collegium Medicum in Bydgoszcz, Nicolaus Copernicus University, Biophysics Department. Her field of research is optical analysis of aggregation of human erythrocytes, especially the first stage of this process.

Maciej Bosek received his PhD degree in biophysics from Nicolaus Copernicus University, Faculty of Physics, Astronomy and Informatics in 2006. Currently, he is a research scientist at Ludwik Rydygier Collegium Medicum, Nicolaus Copernicus University, Biophysics Department. Now his research area covers the optical investigations of processes accompanying the red blood cell (RBC) aggregate creation and sedimentation.

Bronisław Grzegorzewski is a professor and he is head of the chair of biophysics at the Ludwik Rydygier Collegium Medicum in Bydgoszcz, Nicolaus Copernicus University, where he received his PhD degree in 1982. In recent years, he has been focusing on red blood cell aggregation.